Theoretical study on nonlinear optical properties of metalloporphyrin using elongation method

ARTICLE *in* THEORETICAL CHEMISTRY ACCOUNTS · MARCH 2010

Impact Factor: 2.23 · DOI: 10.1007/s00214-009-0669-y

Theor Chem Acc (2010) 125:511–520
DOI 10.1007/s00214-009-0669-y

REGULAR ARTICLE

Theoretical study on nonlinear optical properties of metalloporphyrin using elongation method

Li Kai Yan · Anna Pomogaeva · Feng Long Gu · Yuriko Aoki

Received: 28 August 2009 / Accepted: 20 October 2009 / Published online: 14 November 2009

Abstract A quantum-chemical analysis of the central metal effect on the (hyper)polarizabilities of *meso-meso*-linked metalloporphyrin (MP) oligomers was carried out using elongation finite-field (ELG-FF) method. It is found that *meso-meso*-linked MPs exhibit evident evolution of the third-order nonlinear optical (NLO) response (γ) along with an increasing number of porphyrin units *N*. The order of γ values is as following: $\gamma_{Mg} > \gamma_{Zn} > \gamma_{Ni}$. In contrast to the polarizability, the γ values of *meso-meso*-linked MPs are sensitive to the metals, that is, the nature of the metal can influence the third-order NLO response of MPs. However, the band structures for three MPs are similar to each other, and the differences on the band gaps of three MPs are very small. The local density of states (LDOSs) shows that the central metal gives the significant contributions for unoccupied bands in *meso-meso*-linked MPs.

Keywords Elongation method · Porphyrin · Nonlinear optical properties

Dedicated to Professor Sándor Suhai on the occasion of his 65th birthday and published as part of the Suhai Festschrift Issue.

L. K. Yan · F. L. Gu · Y. Aoki (✉)
Department of Material Sciences,
Faculty of Engineering Sciences, Kyushu University,
Kasuga, Fukuoka 816-8580, Japan
e-mail: aoki@mm.kyushu-u.ac.jp

A. Pomogaeva
Department of Molecular and Material Sciences,
Interdisciplinary Graduate School of Engineering Sciences,
Kyushu University, Kasuga, Fukuoka 816-8580, Japan

Y. Aoki
Japan Science and Technology Agency, CREST,
4-1-8 Hon-chou, Kawaguchi, Saitama 332-0012, Japan

1 Introduction

Nonlinear optics is playing a major role in the light-intensity-dependent transmission properties of materials and the technology photonics. During the last two decades, there has been a great deal of effort on NLO responses of conjugated organic molecules and polymers both from a fundamental perspective and their potential utility in various photonic applications [1–9]. Materials with large third-order optical susceptibility, $\chi^{(3)}$, have numerous applications in NLO. In recent years, a great deal of attention has been paid to the third order NLO properties of organic π-conjugated compounds because of their large second hyperpolarizabilities (γ) and the ultrafast response. The studies on these third-order NLO systems have revealed several tuning parameters of the amplitude and sign of γ, including the π-conjugation length, the bond length alternation, the strength of donor/acceptor substituents, and the charge [10–12]. In the search for improved third-order nonlinearity materials, porphyrins have attracted much attention as an organic material with a large nonlinear optical susceptibility because not only of the large π-electron system with 2D conjugated molecular structure but also of the presence of 1D delocalized electrons.

Recently, a significant improvement in electronic communication between porphyrin pigments can be achieved by β-to-β, *meso*-to-β, and *meso*-to-*meso* linkage topologies [13, 14]. Among these topologies, *meso-meso*-linked porphyrin arrays have emerged as a result of their favorable features, including a linear rodlike shape, ample electronic interactions for rapid incoherent energy hopping, and a lack of an energy sink that disrupts the energy flow along the arrays [15–19]. These properties originate from the orthogonal conformation of the arrays, which tends to minimize the electronic interaction between the neighboring

porphyrins. Elongation of conjugation through *meso*-carbon positions in longer porphyrin arrays induces electronic perturbations to produce a lot of conformers at ambient temperature [20–22].

Metalloporphyrins (MPs) play an important role in biological systems where they serve as active species with the ability to bind ligands, facilitate light-harvesting photosynthetic reactions, transfer electrons, and catalyze enzymatic reactions. MPs, with their extensive π-conjugation, may be used to design new NLO materials. Therien and co-workers [23, 24] first reported the high second order NLO response of the Zn(II) and Cu(II) complexes of 5-X-15-Y-10, 20-diphenylporphyrin ($X = 4\text{-}Me_2NC_6H_4C \equiv C–$; $Y = 4\text{-}NO_2C_6H_4C \equiv C–$). Recently, 5,15-bis(azulenylethynyl) Zn(II) porphyrins either symmetrical or asymmetrical with high TPA cross sections have also been reported [25].

MP oligomers such as zinc(II) complexes are especially versatile, as coordination of pyridine and imidazole ligands to the zinc atom facilitates the self assembly of supramolecular structures [26–28]. The *meso-meso*-linked porphyrin arrays have now reached a discrete 128-mer with a molecular length of approximately 108 nm [29]. Although the π-electron delocalization is disrupted in *meso-meso*-linked porphyrin because of the orthogonal arrangement of neighboring porphyrin units, they exhibit the splitting of the Soret band with the systematic increase of the energy separation with the increase of the number of the linked porphyrins [30].

Along with the development of experimental achievements, the ab initio method or density functional theory (DFT) calculations were carried on porphyrin monomers and dimers [31–34]. There are very few works based on porphyrin trimer by DFT [35]. To our best knowledge, no ab initio studies of porphyrin polymer more than trimer have been performed. In the present study, we report a systematic study of the NLO properties on MPs, where P stands for the porphyrin ligand without any metal; M designates as the metal Mg, Zn, and Ni. The role played by the central metal electronic structure in determining the NLO properties was investigated using ab initio method. The main aim of this work is twofold (1) To clarify the relationship between the structures of porphyrin arrays and their third-order NLO responses. (2) To provide the description on the role of the central metal in MPs.

2 Method

2.1 Elongation finite-field method

Details of the Hartree–Fock elongation method and its application to a system perturbed by an uniform static electric field have been described in the previous papers [36–38]. In this section, we present a brief overview. In the elongation procedure, the delocalized canonical molecular orbitals of a starting cluster are first localized into frozen and active regions in specified parts of the system. Next, a monomer is attached to this cluster to the active region, and the eigenvalue problem is solved by disregarding the regional localized molecular orbitals [39] (RLMOs) which have no or very weak interaction with the attacking monomer. By repeating this procedure, the polymer chain is elongated step by step to any desired length. The obvious advantage of the approach lies in the fact that one can avoid solving very large secular equations for the whole system. The RLMO representation, by which the elongation method is working on, allows one to freeze one part of the system far away from the polymer chain propagation site. The frozen part is disregarded in the elongation self-consistent field procedure. This reduces the number of variational degrees of freedom, and most importantly, the number of two-electron integrals that have to be evaluated in the system can be drastically reduced. Thus, a significant reduction in computation time can be achieved.

To get (hyper)polarizabilities for each elongation step, the above-described elongation method is implemented using the field-dependent Fock matrix,

$$F(E) = H - E \times r + P(E)[2J - K] \tag{1}$$

In Eq. 1, E is the static electric field, H is the core Hamiltonian matrix, r is the vector sum of dipole moment matrices, $P(E)$ is the field-dependent density matrix, and J and K are coulomb and exchange supermatrices. The total energy of a system in the presence of the electric field can be written as a power series of the field magnitude

$$W(E) = W(0) - \mu_i E_i - (1/2!)\alpha_{ij}E_iE_j - (1/3!)\beta_{ijk}E_iE_jE_k - (1/4!)\gamma_{ijkl}E_iE_jE_kE_l + \cdots \tag{2}$$

where $W(0)$ is the field-free total energy and i, j, k, and l are Cartesian axes and the usual summation convention is used for repeated indices. When numerical differentiation is carried out, the molecular (hyper)polarizability tensors are evaluated as

$$\begin{aligned} \alpha_{ij} &= -\left[\partial^2 W(E)/\partial E_i \partial E_j\right]_{E=0} \\ \beta_{ijk} &= -\left[\partial^3 W(\mathrm{E})/\partial E_i \partial E_j \partial E_k\right]_{E=0} \\ \gamma_{ijkl} &= -\left[\partial^4 W(E)/\partial E_i \partial E_j \partial \mathrm{E_k} \partial E_l\right]_{E=0} \end{aligned} \tag{3}$$

As 1D systems are considered in this work, the longitudinal component is most important. Let us suppose that the axis along the chain is z, and then the expressions of the diagonal elements of molecular (hyper)polarizabilities are shown in the following way:

$$\alpha_{zz} = \frac{1}{E_z^2}\left\{\frac{5}{2}W(0) - \frac{4}{3}[W(+E_z) + W(-E_z)] + \frac{1}{12}[W(+2E_z + W(-2E_z))]\right\}$$
$$\beta_{zzz} = \frac{1}{E_z^3}\left\{[W(+E_z) - W(-E_z)] - \frac{1}{2}[W(+2E_z) - W(-2E_z)]\right\} \quad (4)$$
$$\gamma_{zzzz} = \frac{1}{E_z^4}\{-6W(0) - 4[W(+E_z) + W(-E_z)] - [W(+2E_z) + W(-2E_z)]\}$$

In this work, the total energy is obtained using the elongation method. The elongation calculations are performed on each field $E = -2E_z$, $-E_z$, 0, $+E_z$, $+2E_z$ separately, and α_{zz} and γ_{zzzz} are calculated for every elongation step by Eq. 4.

2.2 Methodology for energy band

The crystal orbitals (COs) of a periodic system, as a linear combination of Bloch waves, are delocalized along a polymer with wave vector k. If finite oligomer is long enough, its molecular orbitals (MOs) should be properly delocalized along the chain as well. It becomes possible for every state of an oligomer to assign an appropriate wave vector [40]. The k-values for the states of the chain are defined by

$$k = \frac{q}{M+1}\frac{\pi}{a}, \quad q = 1, 2, \ldots, M, \; 0 < k < \frac{\pi}{a} \quad (5)$$

where M is the number of repeated units of the oligomer and a is the translation vector. For the particular MO, the wave vector could be assigned by projecting the ab initio calculated MO onto real linear combinations of a model CO.

$$X_q^r = \sum_j C_{jr} \sum_{j'} \sin\left(\frac{\pi j' q}{M+1}\right)\left\langle x_j^r \middle| x_{j'}^r \right\rangle,$$
$$Y_q^r = \sum_j C_{jr} \sum_{j'} \cos\left(\frac{\pi j' q}{M+1}\right)\left\langle x_j^r \middle| x_{j'}^r \right\rangle \quad (6)$$

here C_{jr} are MO's expansion coefficients over a set of atomic orbitals X_j^r (AOs), where r is the AO in the jth unit. As a result, k-value is determined by q in Eq. 5 which maximizes the following function

$$R_q = \sum_r \sqrt{\left(X_q^r\right)^2 + \left(Y_q^r\right)^2} \quad (7)$$

while k-values are determined for every MO, the band structure could be formed on the points of the reciprocal space by approximation with smooth curves and proper extrapolation to the edge of the first Brillouin zone.

The method for building band structure from finite chain calculation is accommodated for the elongation method [41], which is developed for accurate calculations of huge molecular systems with time and memory advantages compared to conventional calculations. It helps to reduce disadvantages of the finite cluster calculations.

3 Computational details

In order to investigate the effect of the central metals on the NLO properties of porphyrin polymers, three *meso-meso*-linked MPs are studied in detail and their structures are illustrated in Fig. 1. Herein, the dihedral angle (θ) between adjacent porphyrin units is 90°, and the central metals are Mg, Zn, and Ni, respectively. According to the central metals, three MPs are named as Mg–P, Zn–P, and Ni–P (P = Porphyrin ligand), respectively. The structures of MP polymers are optimized in absence of the external field at B3LYP/6-31G using Gaussian 03 program [42]. The Hartree–Fock (HF) method at ab initio level is employed for the calculation of molecular (hyper)polarizabilities and band structures using General Atomic and Molecular Electronic Structure System (GAMESS) software [43]. 6-31G basis set is used to describe the C, N, and H atoms. To take into account the relativistic effect, the effective core potential (ECP) [44] with corresponding valence double zeta (VDZ) basis set [45–48] is employed for the metals. For (hyper)polarizability calculations, the magnitudes of the external field are fixed to $E = -0.002$, -0.001, 0.000, $+0.001$, and $+0.002$ a.u. and Eq. 4 was used.

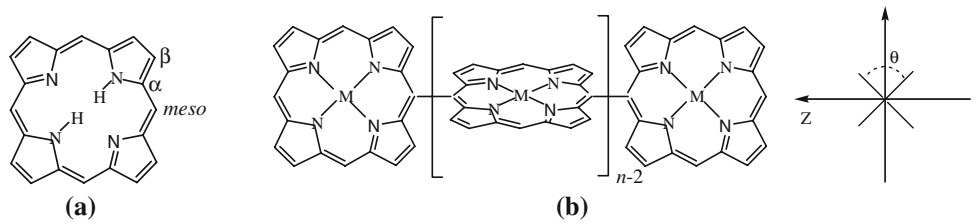

Fig. 1 **a** The molecular structure of porphyrin, with carbon atoms C_α, C_β, and C_{meso} labeled. **b** Molecular structure and axis definition for MPs (M = Mg, Zn, and Ni) arrays (A dihedral angle between adjacent porphyrin units, C_α–C_{meso}–C_{meso}–C_α is defined as θ)

4 Results and discussion

4.1 Reliability of the elongation-FF method

In the previous papers [49, 50], the reliability of the elongation-FF method for (hyper)polarizabilities was confirmed. The total energies under each electric field $E = -0.002$, -0.001, 0.000, $+0.001$, and $+0.002$ a.u. are compared between the conventional and the elongation-FF methods to confirm the reliability of the elongation method. The total energies of Mg–P by elongation and conventional method are listed in Table 1. The difference in the total energy between the elongation and conventional calculations, that is, $\Delta E_{\text{total}} = E_{\text{total}}$ (elongation) $- E_{\text{total}}$ (conventional), and the total energy error per atom, that is, ΔE_{total} per atom $= \Delta E_{\text{total}}$/number of atoms are listed in Table 1. From Table 1, the differences of the total energies per atom under each electric field are within the order of 10^{-8} a.u. for Mg–P. These results demonstrate the reliability of the elongation-FF method for metalloporphyrins.

4.2 Polarizability and second-order hyperpolarizabilities of *meso-meso*-linked MPs

The first hyperpolarizability (β) is negligible due to the symmetry of the systems and thus not treated. The polarizability and second-order hyperpolarizability components of *meso-meso*-linked MPs along the main axis are much larger than those along other directions, therefore only the diagonal elements along the main axis of molecular polarizability, α_{zz}, and second-order hyperpolarizabilities, γ_{zzzz}, are considered in this work. The α_{zz} and $\Delta\alpha = \alpha_N - \alpha_{N-1}$ of three MPs against N are shown in Fig. 2. It can be seen that the order of α_{zz} is as following: $\alpha_{\text{Mg}} > \alpha_{\text{Zn}} > \alpha_{\text{Ni}}$. The difference of α_{zz} between Mg–P and Zn–P is 32.09 a.u. at $N = 4$, and 260.66 a.u. at $N = 22$. For Zn–P and

Table 1 The elongation error in total energy (in a.u.) compared to the conventional calculations for each electric field (in a.u.) at HF level for the starting cluster $N = 4$ of Mg–P

N	E_{total} (conventional)	E_{total} (elongation)	$\Delta E^{\text{a}}_{\text{total}}$	ΔE_{total} per atom[b]
$E = 0.000$				
4	−3,927.0790362013	−3,927.0790362023	−1.000*E*-09	−7.042*E*-12
5	−4,908.5580546429	−4,908.5580531303	1.513*E*-06	8.546*E*-09
6	−5,890.0370723972	−5,890.0370692955	3.102*E*-06	1.463*E*-08
7	−6,871.5160902751	−6,871.5160854713	4.804*E*-06	1.945*E*-08
8	−7,852.9951076808	−7,852.9951011258	6.555*E*-06	2.324*E*-08
$E = 0.001$				
4	−3,927.0803760150	−3,927.0803760151	−9.959*E*-11	−7.013*E*-13
5	−4,908.5598118176	−4,908.5598101607	1.657*E*-06	9.361*E*-09
6	−5,890.0392524007	−5,890.0392487430	3.658*E*-06	1.725*E*-08
7	−6,871.5186959843	−6,871.5186903226	5.662*E*-06	2.292*E*-08
8	−7,852.9981408394	−7,852.9981331212	7.718*E*-06	2.737*E*-08
$E = -0.001$				
4	−3,927.0803760175	−3,927.0803760171	3.997*E*-10	2.815*E*-12
5	−4,908.5598117848	−4,908.5598102726	1.512*E*-06	8.544*E*-09
6	−5,890.0392523938	−5,890.0392491635	3.230*E*-06	1.524*E*-08
7	−6,871.5186959662	−6,871.5186910658	4.900*E*-06	1.984*E*-08
8	−7,852.9981408407	−7,852.9981342800	6.561*E*-06	2.326*E*-08
$E = 0.002$				
4	−3,927.0843981513	−3,927.0843981493	2.000*E*-09	1.408*E*-11
5	−4,908.5650874234	−4,908.5650854111	2.012*E*-06	1.137*E*-08
6	−5,890.0457978979	−5,890.0457931756	4.722*E*-06	2.228*E*-08
7	−6,871.5265207629	−6,871.5265130004	7.762*E*-06	3.143*E*-08
8	−7,853.0072504581	−7,853.0072393820	1.108*E*-05	3.928*E*-08
$E = -0.002$				
4	−3,927.0843981503	−3,927.0843981461	4.200*E*-09	2.958*E*-11
5	−4,908.5650873642	−4,908.5650856764	1.688*E*-06	9.536*E*-09
6	−5,890.0457978985	−5,890.0457940926	3.806*E*-06	1.795*E*-08
7	−6,871.5265206790	−6,871.5265145444	6.135*E*-06	2.484*E*-08
8	−7,853.0072504765	−7,853.0072417952	8.681*E*-06	3.078*E*-08

[a] Total energy difference between elongation and conventional calculations, that is, $\Delta E^{\text{a}}_{\text{total}} = E_{\text{total}}$ (elongation) $- E_{\text{total}}$ (conventional)

[b] Total energy error per atom, that is, ΔE_{total} per atom $= \Delta E_{\text{total}}$/number of atoms

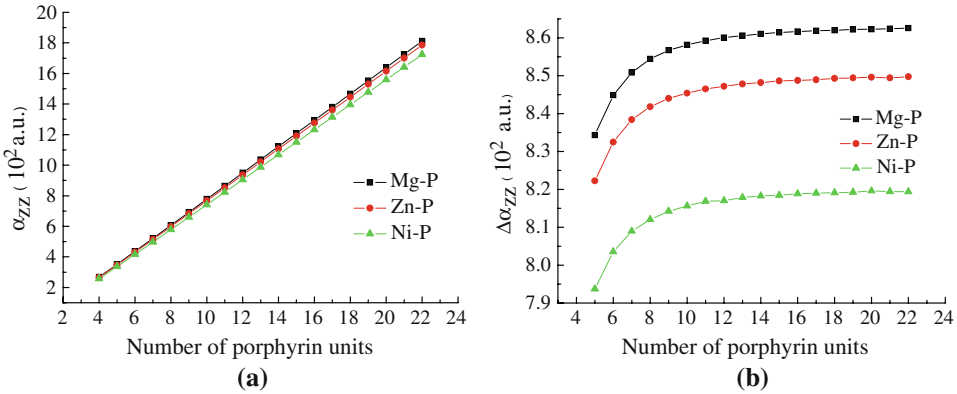

Fig. 2 The dependence of molecular polarizabilities on the number of units. **a** α, **b** $\Delta\alpha$

Ni–P, the α_{zz} difference between two MPs is 80.84 a.u. at $N = 4$, and 617.55 a.u. at $N = 22$. So the metal can influence the molecular polarizability of MPs. For each MP, the value of α_{zz} is increased with the increasing of porphyrin units.

One of the desirable features of porphyrins is optical property due to large hyperpolarizability. Figure 3 shows the dependence of second-order hyperpolarizabilites (γ) and $\Delta\gamma = \gamma_N - \gamma_{N-1}$ on the number of porphyrin units for MPs. It is found that *meso-meso*-linked MPs exhibit evident evolution of the γ_{zzzz} values along with an increasing number of porphyrin units N. For Mg–P, the γ_{zzzz} value is increased from 5.38×10^6 a.u. in 4 units to 69.84×10^6 a.u. in 22 units, 4.85×10^6 a.u. in 4 units of Zn–P is increased to 65.51×10^6 a.u. in 22 units, while for Ni–P, the γ_{zzzz} value is increased from 4.16×10^6 a.u. in 4 units to 58.52×10^6 a.u. in 22 units. The second-order hyperpolarizability is significantly changed according to the central metal. The order of γ_{zzzz} values is as following: $\gamma_{Mg} > \gamma_{Zn} > \gamma_{Ni}$. It suggests that the γ_{zzzz} values of *meso-meso*-linked MPs are sensitive to the metals, that is, the nature of the central metal can significantly influence the γ_{zzzz} values of MPs.

The values of $\Delta\gamma$ show the strong fluctuation due to the numerical instability in high order derivatives of total energy. The deviation was not improved even if the different electric fields were applied. This is because of errors in various numerical procedures that are involved, such as convergence of SCF and CPHF iterations as well as numerical differentiation [51]. Thus this is not only from elongation method, which has been proved a very useful tool to treat large systems [38]. On other hand, the deviations on $\Delta\gamma$ are small and can be accepted as the heavy transition metals are included in the MPs.

4.3 Electronic properties of MP monomers

Before discussing the band structures for three MPs we analyze the electronic structures of MP monomers. To better understand the metal effect on the electronic properties of MPs, the interactions between porphyrin ligand and metalloporphyrins are examined from the frontier molecular orbitals (FMOs), and presented in Fig. 4, which were obtained from HF/6-31G level using Guassian 03. The selected FMOs of MPs are presented in Fig. 5. In going from Mg–P, Zn–P to Ni–P, the HOMO-LUMO gap increases from 6.36, 6.41 to 6.43 eV, and the difference between each other is small. It predicts that the metals Mg, Zn, and Ni might not significantly influence on the electronic structures of MPs in this study.

It is known that porphyrin has been described by four-orbital model of Gouterman [40], which assumes that HOMO (a_u) and HOMO-1 (a_u) are almost degenerate in energy and well separated from the other levels, while the LUMO (b_g) and LUMO + 1 (b_g) are quasi-degenerate

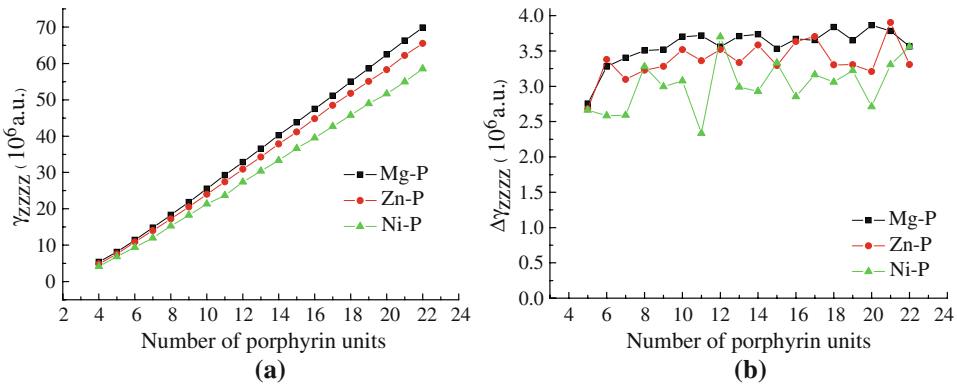

Fig. 3 The dependence of molecular second-order hyperpolarizabilities on the number of units. **a** γ, **b** $\Delta\gamma$

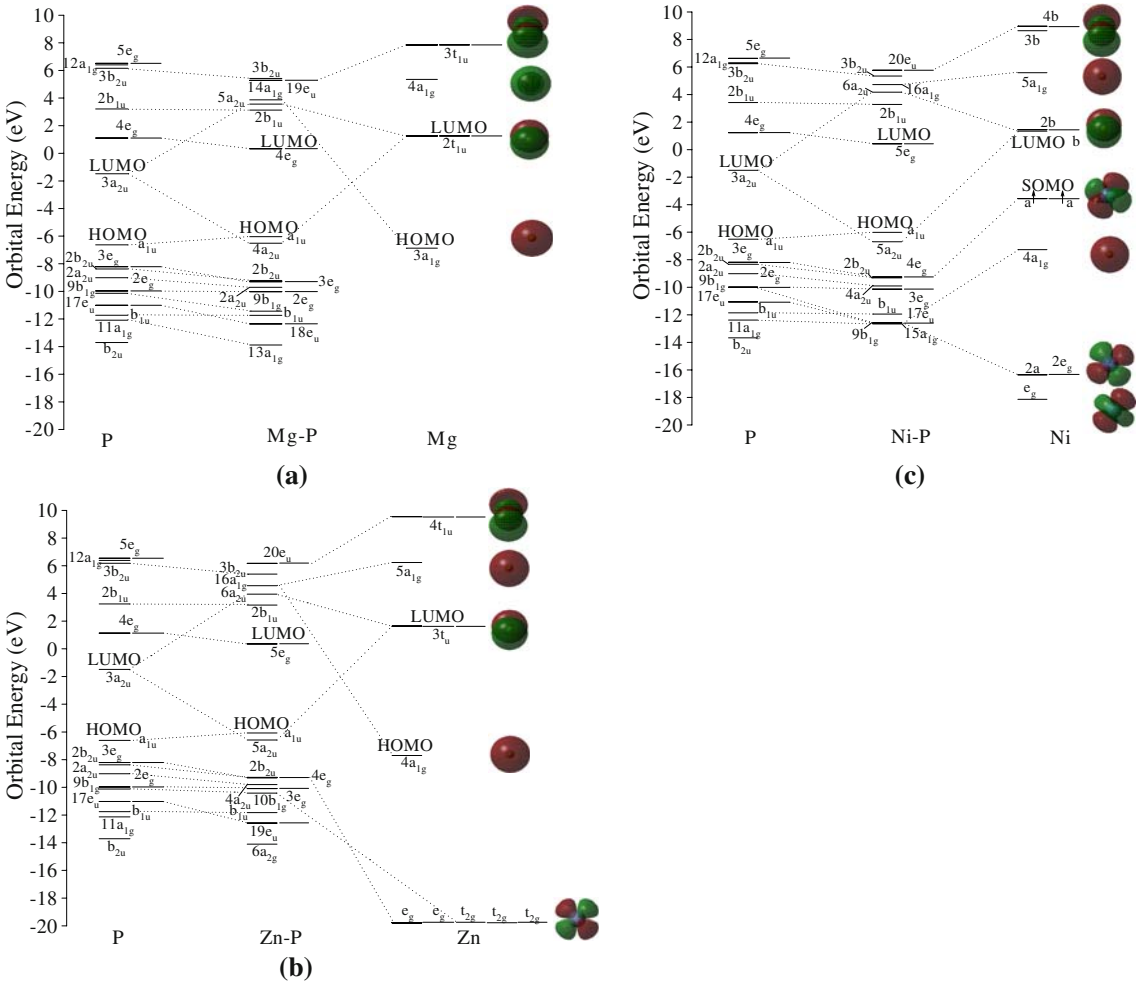

Fig. 4 The orbital energy levels of porphyrin (P) and Mg–P (**a**), Zn–P (**b**), and Ni–P (**c**)

orbitals. In Mg–P, HOMO (a_{1u}) and HOMO-1 ($4a_{2u}$) are separated by 0.48 eV; LUMO ($4e_g$) are degenerate orbitals, and separated from LUMO + 1 ($2b_{1u}$) by 2.80 eV. The HOMO (a_{1u}) in Mg–P originates from the corresponding orbital of ligand P, while the LUMO ($4e_g$) is from the LUMO + 1 ($4e_g$) of ligand. The HOMO and LUMO distribute over the molecule, and show π and π^* characters, respectively. The HOMO-1 ($4a_{2u}$) has slightly contribution from metal Mg. The metal Mg gives the significant contributions for $5a_{2u}$, $14a_{1g}$, and $19e_u$ of Mg–P. So the metal Mg modifies the unoccupied molecular orbitals in FMOs. The FMOs of Zn-P are similar to those of Mg–P. The HOMO (a_{1u}) and LUMO ($5e_g$) show π and π^* characters, respectively. The main components of $6a_{2u}$, $16a_{1g}$, and $20e_u$ are from the metal Zn, and Zn also mixes with $4e_g$ and $10b_{1g}$ using *d* orbitals. As for Ni–P, the main contributions of Ni are found in $6a_{2u}$, $16a_{1g}$, $20e_u$, $9b_{1g}$, and $15a_{1g}$ orbitals.

From Figs. 4 and 5, it is evident that the LUMO + 1, LUMO, HOMO, and HOMO-1 have the same nature for three MPs, that is, the LUMO + 1 and HOMO are from pure carbon *p* orbitals, and LUMO and HOMO-1 orbitals are from carbon and nitrogen *p* orbitals. As the nature of the FMOs are similar to each other, and the contributions of the metals are negligible near HOMO-LUMO level MOs in all cases, so the difference of HOMO-LUMO gap between three MPs are small.

The orbital natures of three MPs were also analyzed at Hartree–Fock level using GAMESS. The 6-31G basis set is chosen for C, N, and H atoms, and the metals are described by ECP with VDZ basis set. The orbital natures of LUMO+1, LUMO, HOMO, and HOMO-1 for three MPs are same with the calculations at HF/6-31G level using Gaussian 03 software.

The molecular orbitals of three MP dimers are also analyzed and the near HOMO-LUMO energy level is presented in Fig. 6. The HOMO-LUMO energy gap of three dimers increases from Mg–P, Zn–P to Ni–P. However, the differences of HOMO-LUMO gaps between three MP dimers are small. The FMOs of three MP dimers are similar

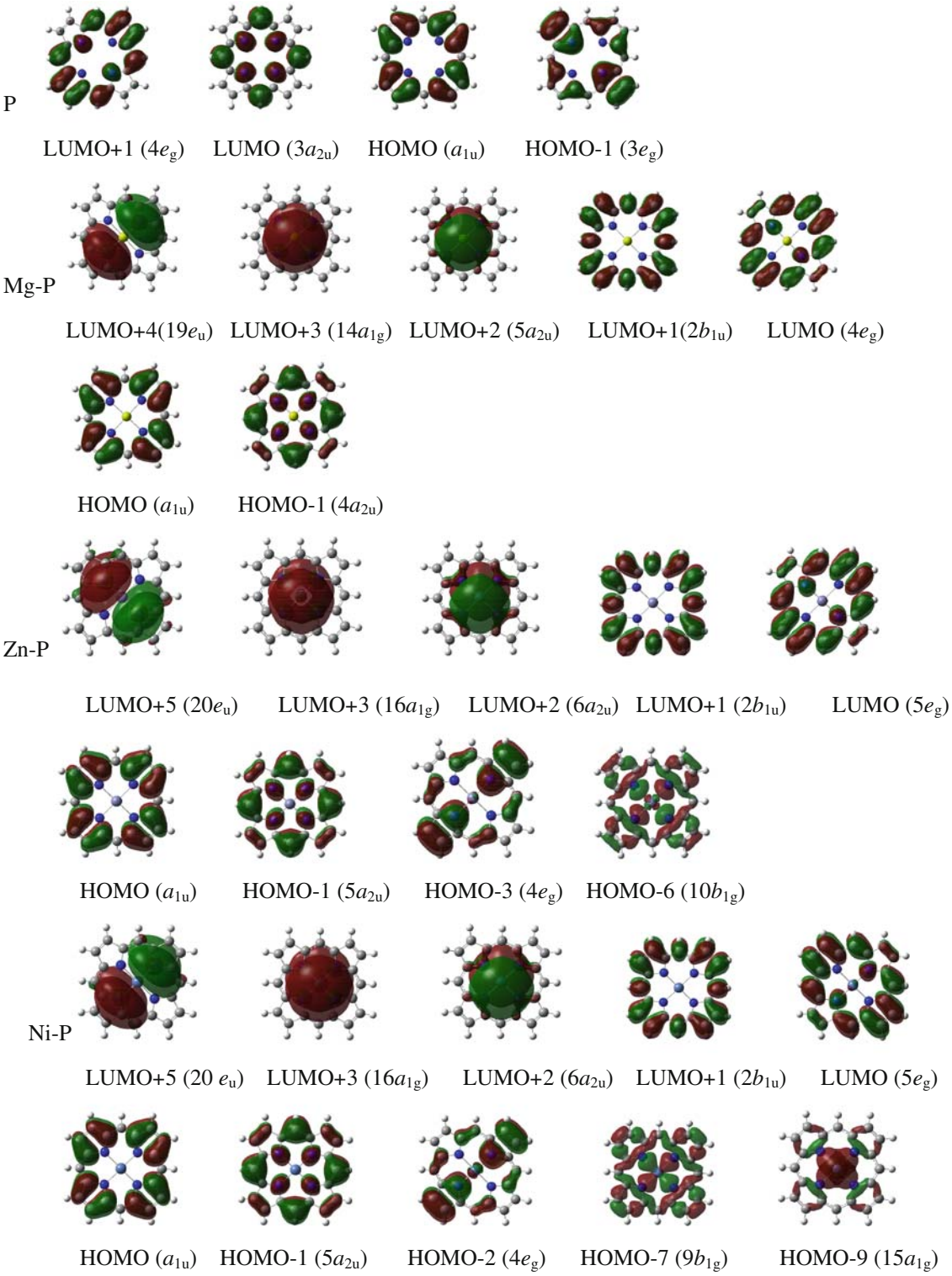

Fig. 5 The molecular orbitals of P, Mg–P, Zn–P, and Ni–P

to each other. Herein, only FMOs of Mg–P are shown in Fig. 7. The HOMO (6a_2) and HOMO-1 (4b_1) in Mg–P dimer are π-orbitals, which are pure carbon p orbitals, while HOMO-2 (41e) are degenerate orbitals, which delocalize on the carbon and nitrogen atoms, and also have slight contributions from the metal. The LUMO (5b_1), degenerate LUMO+1 (42e), and LUMO+2 (7a_2) have the same orbital nature, which are from carbon and nitrogen p orbitals.

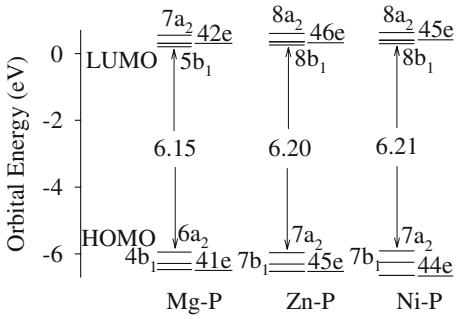

Fig. 6 The frontier molecular orbital level of MP dimers

4.4 Band structures

At this stage, it is worth stressing the behavior of band structures and local density of states (LDOSs). For three MPs, the band structure calculations are obtained from 22 units oligomers by HF method. In the calculations, ECP with VDZ basis set for metals and 6-31G basis set for other atoms. In Fig. 8, we present a plot of the band as a function of k and LDOSs are shown in Fig. 9. The fundamental energy gaps of Mg–P, Zn–P, and Ni–P are 5.76, 5.79, and 5.81 eV, respectively, which are related to the order of γ_{zzzz} values ($\gamma_{Mg} > \gamma_{Zn} > \gamma_{Ni}$). During the band structure calculations, the 22 units oligomers were arranged as 11 units due to the requirement of periodic condition. For Mg–P, the first and second highest valence bands are π-bands, which are from pure carbon p orbitals. These two bands have the same characters with the HOMO ($6a_2$) and HOMO-1 ($4b_1$) of Mg–P dimer. The states of linear one are degenerate, which slightly contains Mg contributions. The linear valence band exactly corresponds to the degenerate HOMO-2 ($41e$) of Mg–P dimer. The three lowest conduction bands are π^*-bands, which are from carbon and nitrogen p orbitals. The linear conduction band is also degenerate. It can be seen that the first three conduction bands are in agreement with the unoccupied molecular orbital nature of Mg–P dimer. The behaviors of Zn–P and Ni–P are very similar to that of Mg–P. From Mg–P, Zn–P to Ni–P, the degenerate linear valence band shifts down. Due to symmetry, the bands should be pairwise degenerate at point $\chi = \pi/a$. However, there is a small error since the energies at the edges of the Brillouin zone are obtained by extrapolation [40].

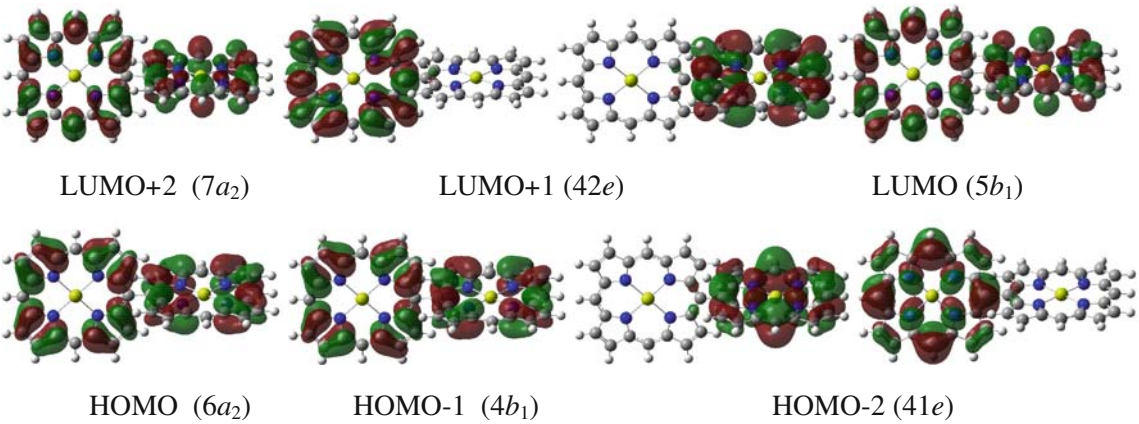

Fig. 7 The frontier molecular orbitals of Mg–P dimer

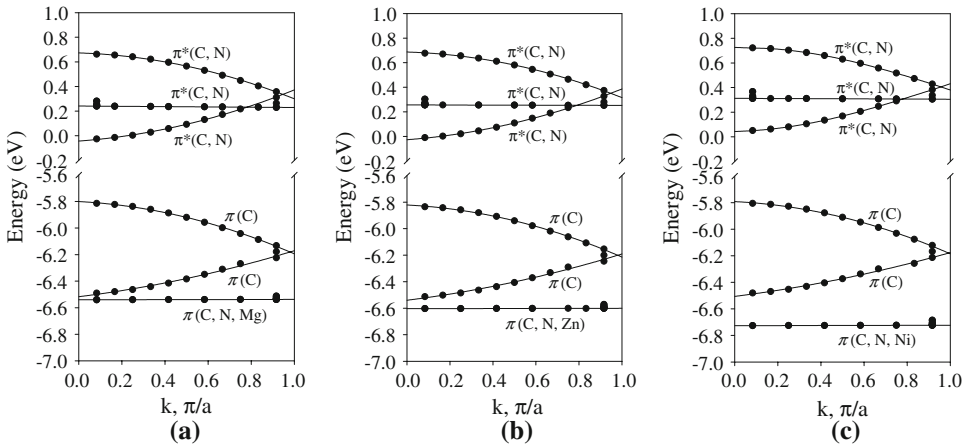

Fig. 8 Band structures of MP polymers extracted from elongation HF/6-31 (ECP/DVZ for metals) calculations of 22 units. **a** Mg–P, **b** Zn–P, **c** Ni–P

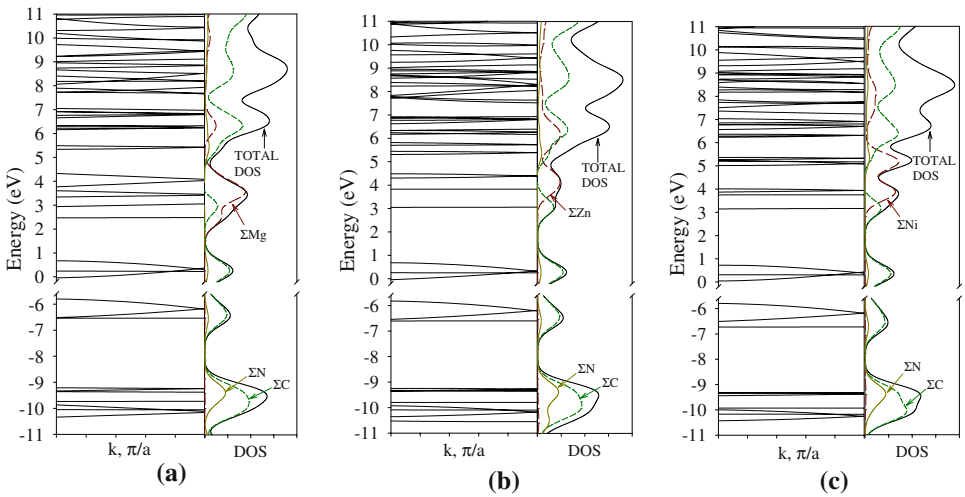

Fig. 9 Band structures and LDOSs for MP polymers extracted from elongation HF/6-31G (ECP/VDZ for metals) calculations of 22 units oligomers. For LDOS, *black lines* are total DOS; *red dash lines*, *yellow lines*, and *green dash lines* are metal, nitrogen, and carbon LDOS contributions, respectively. **a** Mg–P, **b** Zn–P, **c** Ni–P

To understand the electronic structures, the LDOSs were examined for three MP polymers by elongation calculation. For each MP, the first three valence bands and three conduction bands have the main contributions from carbon orbitals. The metals give the significant contributions for unoccupied bands, which are in agreement with the investigations of their monomers and dimers. The LDOS for three MPs are similar to each other.

5 Conclusion

In this article, we showed the effectiveness and efficiency of the elongation method for calculating *meso-meso*-linked metalloporphyrins. The central metal effect and chain length dependence of α_{zz} and γ_{zzzz} on *meso-meso*-linked MPs are examined at ab initio levels by the elongation-FF method. The total energy error was in the order of 10^{-8} hartree/atom for three MPs. The α_{zz} values for each MP are increased with the increasing porphyrin units by 6 times from 4 units to 22 units. While three MPs exhibit evident evolution of the third-order NLO response (γ) along with an increasing number of porphyrin units *N*. For three MPs, the γ_{zzzz} value in 22 units is found to be 13 times as large as that of 4 units. In contrast to the polarizability, second-order hyperpolarizability of *meso-meso*-linked MPs are more sensitive to the metals, that is, the γ values are affected by changing the central metal. The order of γ_{zzzz} values is according to $\gamma_{Mg} > \gamma_{Zn} > \gamma_{Ni}$. The band structures are similar to each other and LDOSs show that the metals give the significant contributions to unoccupied bands, which are in agreement with the molecular orbital natures of monomers and dimers.

Acknowledgments This work was supported by the Japan Society for the Promotion of Science for a JSPS fellowship.

References

1. Brédas JL, Adant C, Tackx P, Persoons A (1994) Chem Rev 94:243
2. Geskin VM, Lambert C, Brédas JL (2003) J Am Chem Soc 125:15651
3. Nakano M, Kishi R, Ohta S, Takahashi H, Kubo T, Kamada K, Ohta K, Botek E, Champagne B (2007) Phys Rev Lett 99:033001
4. Keinan S, Therien MJ, Beratan DN, Yang W (2008) J Phys Chem A 112:12203
5. An Z, Wong KYJ (2001) Chem Phys 114:1010
6. Kim TD, Kang JW, Luo J, Jang SH, Ka JW, Tucker N, Benedict JB, Dalton LR, Gray T, Overney RM, Park DH, Herman WN, Jen AKY (2007) J Am Chem Soc 129:488
7. Kang H, Evmenenko G, Dutta P, Clays K, Song K, Marks TJ (2006) J Am Chem Soc 128:6194
8. Ohnishi S, Orimoto Y, Gu FL, Aoki Y (2007) J Chem Phys 127:084702
9. Sung JY, Silbey RJ (2003) J Chem Phys 118:2443
10. Fukui H, Kishi R, Minami T, Nagai H, Takahashi H, Kubo T, Kamada K, Ohta K, Champagne B, Botek E, Nakano M (2008) J Phys Chem A 112:8423
11. Nakano M, Shigemoto I, Yamada S, Yamaguchi K (1995) J Chem Phys 103:4175
12. Oliveira LN, Amaral OAV, Castro MA, Fonseca TL (2003) Chem Phys 289:221
13. Kumble R, Palese S, Lin VSY, Therien MJ, Hochstrasser RM (1998) J Am Chem Soc 120:11489
14. Beljonne D, O'Keefe GE, Hamer PJ, Friend RH, Anderson HL, Brédas JL (1997) J Chem Phys 106:9439
15. Tsuda A, Osuka A (2001) Science 293:79
16. Tsuda A, Nakano A, Furuta H, Yamochi H, Osuka A (2000) Angew Chem Int Ed 39:558
17. Osuka A, Shimidzu H (1997) Angew Chem Int Ed Engl 36:135
18. Ogawa T, Nishimoto Y, Yoshida N, Ono N, Osuka A (1999) Angew Chem Int Ed 38:176
19. Ahn TK, Yoon ZS, Hwang IW, Lim JK, Rhee H, Joo T, Sim F, Kim SK, Aratani N, Osuka A, Kim D (2005) J Phys Chem B 109:11223
20. Rubtsov IV, Susumu K, Rubtsov GI, Therien MJ (2003) J Am Chem Soc 125:2687
21. Shediac R, Gray MHB, Uyeda HT, Johnson RC, Hupp JT, Angiolillo PJ, Therien MJ (2000) J Am Chem Soc 122:7017

22. Duncan TV, Rubtsov IV, Uyeda HT, Therien MJ (2004) J Am Chem Soc 126:9474
23. LeCours SM, Guan HW, DiMagno SG, Wang CH, Therien MJ (1996) J Am Chem Soc 118:1497
24. Karki L, Vance FW, Hupp JT, LeCours SM, Therien MJ (1998) J Am Chem Soc 120:2606
25. Kim KS, Noh SB, Katsuda T, Ito S, Otsuka A, Kim D (2007) Chem Commun 2479–2481. doi:10.1039/b704986b
26. Hwang IW, Kamada T, Ahn TK, Ko DM, Nakamura T, Tsuda A, Osuka A, Kim D (2004) J Am Chem Soc 126:16187
27. Hwang IW, Cho HS, Jeong DH, Kim D, Tsuda A, Nakamura T, Osuka A (2003) J Phys Chem B 107:9977
28. Anderson HL (1994) Inorg Chem 33:972
29. Aratani N, Osuka A, Kim YH, Jeong DH, Kim D (2000) Angew Chem Int Ed 39:1458
30. Ohta N, Iwaki Y, Ito T, Yamazaki I, Osuka A (1999) J Phys Chem B 103:11242
31. Johansson MP, Sundholm D, Gerfen G, Wikström M (2002) J Am Chem Soc 124:11771
32. Kelley RF, Tauber MJ, Wasielewski MR (2006) J Am Chem Soc 128:4779
33. Praneeth VKK, Neese F, Lehnert N (2005) Inorg Chem 44:2570
34. Liao MS, Watts JD, Huang MJ (2007) J Phys Chem A 111:5927
35. Ray PC, Bonifassi P, Leszczynski J (2008) J Phys Chem A 112:2870
36. Imamura A, Aoki Y, Maekawa K (1991) J Chem Phys 95:5491
37. Aoki Y, Imamura A (1992) J Chem Phys 97:8432
38. Gu FL, Aoki Y, Imamura A, Bishop DM, Kirtman B (2003) Mol Phys 101:1487
39. Gu FL, Aoki Y, Korchowiec J, Imamura A, Kirtman B (2004) J Chem Phys 121:10385
40. Pomogaeva A, Kirtman B, Gu FL, Aoki Y (2008) J Chem Phys 128:074109
41. Pomogaeva A, Springborg M, Kirtman B, Gu FL, Aoki Y (2009) J Chem Phys 130:194106
42. Frisch MJ, Trucks GW, Schlegel HB, Scuseria GE, Robb MA, Cheeseman JR, Montgomery JA Jr, Vreven T, Kudin KN, Burant JC, Millam JM, Iyengar SS, Tomasi J, Barone V, Mennucci B, Cossi M, Scalmani G, Rega N, Petersson GA, Nakatsuji H, Hada M, Ehara M, Toyota K, Fukuda R, Hasegawa J, Ishida M, Nakajima T, Honda Y, Kitao O, Nakai H, Klene M, Li X, Knox JE, Hratchian HP, Cross JB, Bakken V, Adamo C, Jaramillo J, Gomperts R, Stratmann RE, Yazyev O, Austin AJ, Cammi R, Pomelli C, Ochterski JW, Ayala PY, Morokuma K, Voth GA, Salvador P, Dannenberg JJ, Zakrzewski VG, Dapprich S, Daniels AD, Strain MC, Farkas O, Malick DK, Rabuck AD, Raghavachari K, Foresman JB, Ortiz JV, Cui Q, Baboul AG, Clifford S, Cioslowski J, Stefanov BB, Liu G, Liashenko A, Piskorz P, Komaromi I, Martin RL, Fox DJ, Keith T, Al-Laham MA, Peng CY, Nanayakkara A, Challacombe M, Gill PMW, Johnson B, Chen W, Wong MW, Gonzalez C, Pople JA (2004) Gaussian 03, Revision C.02. Gaussian, Inc, Wallingford
43. Schmidt MW, Baldridge KK, Boatz JA, Elbert ST, Gordon MS, Jensen JH, Koseki S, Matsunaga N, Nguyen KA, Su SJ, Windus TL, Dupuis M, Montgomery JA (1993) GAMESS Version 14 (Iowa State University, Iowa, 2003). J Comput Chem 14:1347
44. Dolg M (2003) In: Grotendorst J (ed) Modern methods and algorithms of quantum chemistry. Proceedings, 2nd edn. John von Neumann Institute for Computing, Jülich, NIC Series, vol 3, p 507
45. Binkley JS, Pople JA, Hehre WJ (1980) J Am Chem Soc 102:939
46. Stevens WJ, Basch H, Krauss M (1984) J Chem Phys 81:6026
47. Stevens WJ, Krauss M, Basch H, Jasien PG (1992) Can J Chem 70:612
48. Cundariand TR, Stevens WJ (1993) J Chem Phys 98:5555
49. Ohnishi S, Gu FL, Naka K, Imamura A, Kirtman B, Aoki Y (2004) J Phys Chem A 108:8478
50. Orimoto Y, Gu FL, Imamura A, Aoki Y (2007) J Chem Phys 126:215104
51. Champagne B, Kirtman B (2001) Handbook of advanced electronic and photonic materials and devices, vol 9. Elsevier, p 99